

# Garlic oil supplementation blocks inflammatory pyroptosis-related acute lung injury by suppressing the NF- $\kappa$ B/NLRP3 signaling pathway via H<sub>2</sub>S generation

Tursunay Dilxat<sup>1</sup>, Qiang Shi<sup>1</sup>, Xiaofan Chen<sup>1</sup>, Xuxin Liu<sup>1</sup>

<sup>1</sup>Xinjiang Agricultural Vocational Technological College, Changji 831100, Xinjiang, China

**Correspondence to:** Xuxin Liu; email: [lx529@hotmail.com](mailto:lx529@hotmail.com), <https://orcid.org/0000-0002-3464-6438>

**Keywords:** acute lung injury, garlic oil, lipopolysaccharide, anti-inflammatory

**Received:** October 19, 2023

**Accepted:** March 9, 2024

**Published:** April 12, 2024

**Copyright:** © 2024 Dilxat et al. This is an open access article distributed under the terms of the [Creative Commons Attribution License](https://creativecommons.org/licenses/by/4.0/) (CC BY 4.0), which permits unrestricted use, distribution, and reproduction in any medium, provided the original author and source are credited.

## ABSTRACT

Acute lung injury (ALI) is a major cause of acute respiratory failure with a high morbidity and mortality rate, and effective therapeutic strategies for ALI remain limited. Inflammatory response is considered crucial for the pathogenesis of ALI. Garlic, a globally used cooking spice, reportedly exhibits excellent anti-inflammatory bioactivity. However, protective effects of garlic against ALI have never been reported. This study aimed to investigate the protective effects of garlic oil (GO) supplementation on lipopolysaccharide (LPS)-induced ALI models. Hematoxylin and eosin staining, pathology scores, lung myeloperoxidase (MPO) activity measurement, lung wet/dry (W/D) ratio detection, and bronchoalveolar lavage fluid (BALF) analysis were performed to investigate ALI histopathology. Real-time polymerase chain reaction, western blotting, and enzyme-linked immunosorbent assay were conducted to evaluate the expression levels of inflammatory factors, nuclear factor- $\kappa$ B (NF- $\kappa$ B), NLRP3, pyroptosis-related proteins, and H<sub>2</sub>S-producing enzymes. GO attenuated LPS-induced pulmonary pathological changes, lung W/D ratio, MPO activity, and inflammatory cytokines in the lungs and BALF. Additionally, GO suppressed LPS-induced NF- $\kappa$ B activation, NLRP3 inflammasome expression, and inflammatory-related pyroptosis. Mechanistically, GO promoted increased H<sub>2</sub>S production in lung tissues by enhancing the conversion of GO-rich polysulfide compounds or by increasing the expression of H<sub>2</sub>S-producing enzymes *in vivo*. Inhibition of endogenous or exogenous H<sub>2</sub>S production reversed the protective effects of GO on ALI and eliminated the inhibitory effects of GO on NF- $\kappa$ B, NLRP3, and pyroptotic signaling pathways. Overall, these findings indicate that GO has a critical anti-inflammatory effect and protects against LPS-induced ALI by suppressing the NF- $\kappa$ B/NLRP3 signaling pathway via H<sub>2</sub>S generation.

## INTRODUCTION

Acute lung injury (ALI) is a noncardiogenic acute progressive hypoxic lung disease frequently accompanied by diffuse alveolar injury and acute respiratory failure [1, 2]. Its pathological characteristics include alveolar epithelium injury, increased pulmonary microvessel permeability, exudation, pulmonary edema, and substantial inflammatory cell infiltration [3]. This disease affects millions of people globally and has a high mortality and morbidity rate [1, 4]. Lipopolysaccharide (LPS), one of the most important pathogenic antigens of

gram-negative bacteria, is typically used to establish animal models of ALI to investigate more effective ways to overcome ALI [5, 6]. Despite tremendous progress in understanding the causative mechanisms of the disease, effective therapeutic strategies for patients with ALI remain limited. Therefore, there is an urgent need to explore more methods and drugs to treat ALI.

Although the pathogenic mechanism of ALI remains unclear, the inflammatory response is one of the key mechanisms that has been conclusively shown to cause ALI [7]. In a previous study on a mouse model of ALI,

the levels of tumor necrosis factor alpha (TNF- $\alpha$ ) and interleukin (IL-1 $\beta$ ), as representatives of many inflammatory cytokines, were found to be elevated in bronchoalveolar lavage fluid (BALF) [8]. Additionally, another study reported that LPS-induced ALI was alleviated through the suppression of the expression of numerous inflammatory cytokines [9, 10]. Studies have confirmed that nuclear factor- $\kappa$ B (NF- $\kappa$ B) signaling is a key pathway that regulates the production of these inflammatory cytokines. Suppression of NF- $\kappa$ B signaling attenuated LPS-induced alveolar epithelial cell injury and LPS-induced ALI [11, 12]. The NLRP3 inflammasome that mediates IL-1 $\beta$  and IL-18 maturation also plays a vital role in ALI progression [13]. Pyroptosis is a new type of inflammatory programmed cell death that is activated by NLRP3 and causes the release of multiple gasdermin family members, including gasdermin E (GSDME) and gasdermin D (GSDMD) [14, 15]. Gasdermins, considered as indicators of pyroptosis, are responsible for cell perforation. Pyroptosis also plays a critical role in promoting unfavorable developmental outcomes in ALI inflammation [16, 17]. Consequently, the development of anti-inflammatory and antipyroptotic drugs for treating ALI is preferred.

In the past few years, the role of nutrition in disease prevention and treatment has received rapid attention. Studies have revealed that many active ingredients derived from food can prevent or treat ALI [18, 19]. However, the availability of some ingredients from their natural sources is highly limited. Recently, accumulating evidence has indicated that garlic, a globally used cooking spice, has a myriad of beneficial effects [20, 21]. Garlic exhibits excellent anti-inflammatory bioactivity [22, 23] and inhibits NF- $\kappa$ B activation [24]. Owing to the relatively low cost, remarkable effectiveness, and few side effects, the consumption of garlic has progressively increased worldwide [25]. Additionally, leveraging the therapeutic potential of its bioactive molecules and discovering the underlying mechanism is crucial for reducing healthcare costs and supporting economic development in rural communities.

Research suggests that the large amount of organosulfur compounds that garlic contains, such as diallyl trisulfide (DATS) and diallyl disulfide, is the key to its medicinal value [26, 27]. Ko et al. revealed that garlic oil and diallyl disulfide could prevent cigarette smoke-induced airway inflammation in mice, confirming their therapeutic potential in pulmonary diseases.

H<sub>2</sub>S released from these organic polysulfides under physiological conditions is a key biomaterial in the

regulation of physiological and pathological diseases, which can exert protective effects against ALI through various pathways, such as antioxidant stress, antinitrification stress, anti-inflammation, and anti-ferroptosis [28, 29]. Additionally, GO supplementation has been reported to upregulate the levels of H<sub>2</sub>S-producing enzymes, including cystathionine  $\beta$ -synthase (CBS), cystathionine  $\gamma$ -lyase (CSE), and 3-mercaptopyruvate sulphurtransferase (3MST) [30–32]. H<sub>2</sub>S is involved in respiratory activities and can affect the outcomes of various lung diseases [33]. A previous study revealed that serum levels of H<sub>2</sub>S in patients with chronic obstructive pulmonary disease are lower than those in healthy individuals [34]. Moreover, H<sub>2</sub>S can exert an antioxidation effect by attenuating the levels of glutathione disulfide in the lungs of hypoxia-induced pulmonary hypertensive rats. Furthermore, Wang et al. revealed that H<sub>2</sub>S exerts its antifibrotic activity by suppressing the TGF $\beta$ /Smad pathway [35]. Notably, H<sub>2</sub>S alleviates acute kidney damage by suppressing NLRP3 activation and pyroptosis [36]. Because NLRP3 plays a critical role in ALI inflammation, we speculated whether GO exerts its protective effect against ALI by inhibiting the NF- $\kappa$ B/NLRP3 signaling pathway via H<sub>2</sub>S generation.

Therefore, the present study aimed to investigate the therapeutic effect of GO on LPS-induced ALI and its intrinsic molecular mechanisms in an ALI mouse model.

## MATERIALS AND METHODS

### Mice protocols

Male C57BL/6 mice (6–8 weeks old) were purchased from Karamay Zhonghui Trading Co., Ltd., (Karamay City, China). All trial procedures were approved by The Ethics Committee of Xinjiang Agricultural Vocational Technological College. Mice were randomized into three groups: control, LPS, and LPS + GO (GO, 100 mg/kg); or five groups: control, LPS, LPS + GO (GO, 100 mg/kg) [37, 38], LPS + GO (GO, 100 mg/kg) + iodoacetamide (IAM); LPS + GO (GO, 100 mg/kg) + aminoxyacetic acid ((AOAA), 50 mg/kg) + DL-propargylglycine ((PAG), 100 mg/kg). For ALI model establishment, the mice were anesthetized via intraperitoneal injection of sodium pentobarbital (50 mg/kg) and then intratracheally injected with LPS (5 mg/kg) dissolved in 50  $\mu$ l of phosphate-buffered saline (PBS). An equal volume of PBS was applied to control mice as a control. For GO delivery, mice were intratracheally injected with GO (100 mg/kg, dissolved in 50  $\mu$ l of dimethyl sulfoxide (DMSO)) 4 h before LPS instillation. DATS is an active constituent isolated from GO, and IAM is an effective inhibitor of the conversion of DATS to H<sub>2</sub>S *in vivo*.

For IAM delivery, mice were administered 3% IAM in their drinking water 30 min after LPS instillation. CBS and CSE are the two main enzymes that mediate H<sub>2</sub>S production *in vivo*. AOAA and PAG are CBS and CSE inhibitors, respectively. For AOAA and PAG delivery, mice were intraperitoneally injected with AOAA (50 mg/kg) and PAG (100 mg/kg) 30 min after LPS instillation. Samples were collected 24 h after LPS instillation. Enzyme-linked immunosorbent assay (ELISA), histological analysis, total protein assays, and cell counting were performed with collected BALF samples. ELISA, immunohistochemistry, real-time polymerase chain reaction (PCR), and western blotting were conducted with collected lung tissues.

### Drugs and reagents

The following compounds were used in this study: LPS (cat. L2880, Sigma-Aldrich, USA), GO (cat. W250309, Sigma-Aldrich), IAM (cat. A3221, Sigma-Aldrich), AOAA (cat. C13408, Sigma-Aldrich), and PAG (cat. P7888, Sigma-Aldrich). Antibodies used were IL-6 antibody (cat. 21865-1-AP, Proteintech, China), TNF- $\alpha$  antibody (cat. 60291-1-Ig, Proteintech), IL-1 $\beta$  antibody (cat. 16806-1-AP, Proteintech), IL-18 antibody (cat. 10663-1-AP, Proteintech), p-NF $\kappa$ B p65 antibody (cat. 3033, Cell Signaling Technology, USA), NF- $\kappa$ B p65 antibody (cat. 8242T, Cell Signaling Technology), NLRP3 antibody (cat. 15101S, cat. 8242T, Cell Signaling), ASC antibody (cat. sc-514414, Santa Cruz Biotechnology, USA), cleaved caspase-1 antibody (cat. sc56036, Santa Cruz Biotechnology), GSDMD antibody (cat. A18281, Abclonal, USA), cleaved N-terminal GSDME antibody (cat. ab222407, Abcam, UK), CBS antibody (cat. GTX628777, GeneTex, USA), CSE antibody (cat. 12217-1-AP, Proteintech), 3MST antibody (cat. HPA001240, Sigma-Aldrich), and  $\beta$ -actin antibody (60004-1-Ig, Proteintech).

### Hematoxylin and eosin (H&E) staining and pathology scores

The lungs were fixed with a 12% neutral formaldehyde solution for 24 h and then dehydrated in a series of graded concentrations of alcohol dilutions. The tissue was then embedded in paraffin, and the paraffin blocks were cut into 4- $\mu$ m-thick sections. Sections were stained with H&E and then observed under a light microscope for pathological changes in the lung tissues. The ALI score was independently calculated by two pathologists based on parameters including alveolar septal thickening, pulmonary hemorrhage, hyaline membrane formation, and substantial neutrophil infiltration into alveolar spaces [39]. The scoring scale was defined as follows: virtually no damage, 0–1 point; mild-to-moderate damage, 2–5 points; and severe damage, 5–10 points.

### Detection of lung wet/dry (W/D) ratio

The upper lobe of the left lung was dissected out, immediately measured, and used as the wet weight of the lung. The lung tissue was then dried at 65°C for 72 h, and the weight of the dried lungs was measured immediately. The W/D ratio of the lungs was calculated as an indication of the degree of pulmonary edema.

### Lung myeloperoxidase (MPO) activity measurement

Lung tissues used for MPO experiments must be irrigated with PBS to remove all blood. Lung MPO activity was determined using an MPO colorimetric activity assay kit (cat. ab105136, Abcam). The optical density value of MPO was measured using a microplate reader (FilterMax F5, Molecular Devices, USA) at 460 nm.

### Bronchoalveolar lavage

After being euthanized, the chest cavity of the mice was exposed and the trachea was intubated. An 18G sterile and blunt-ended needle was inserted through the resection port into the trachea. A total volume of approximately 2.4 ml of BALF was recovered from each mouse through injection of 2 ml of cold saline. The supernatants were collected via centrifugation and stored. The total protein level of BALF was measured using a BCA protein assay kit (cat. CW0014S, CWBIO, Jiangsu, China). The precipitated cells were resuspended, and the number of cells in BALF was calculated using a grid blood cell counter.

### RNA extraction and real-time PCR

Total cellular RNA was extracted and reverse transcribed. The cDNA was then subjected to a real-time PCR program running on an ABI7500 Real-Time PCR System (Applied Biosystems, USA) with the following thermocycling conditions: initial predenaturation for 2 min at 50°C and 10 min at 95°C, followed by a 40-cycle two-step PCR (95°C for 15 s and 60°C for 1 min). GAPDH was used as an internal reference control. The primer sequences for the RNAs to be detected are listed in Table 1.

### Western blot

Lung tissue lysate was prepared with RIPA buffer (cat. P0013B, Beyotime, Shanghai, China) using a tissue homogenizer. Proteins were precipitated via centrifugation, followed by denaturation at 95°C for 10 min. After quantification using a BCA protein concentration quantification kit (cat. CW0014S, CWBIO), proteins of different molecular weight sizes were separated via SDS-PAGE

**Table 1. Sequences of PCR primers used in this study.**

GAPDH	Forward (5'–3')	AGGTCGGTGTGAACGGATTG
	Reverse (5'–3')	GGGGTCGTTGATGGCAACA
IL-6	Forward (5'–3')	GGCGGATCGGATGTTGTGAT
	Reverse (5'–3')	GGACCCAGACAATCGGTTG
TNF- $\alpha$	Forward (5'–3')	ACCCTCACACTCACAACCA
	Reverse (5'–3')	ACCCTGAGCCATAATCCCCT
IL-1 $\beta$	Forward (5'–3')	ATGATGGCTTATTACAGTGGCAA
	Reverse (5'–3')	GTCGGAGATTTCGTAGCTGGA
IL-18	Forward (5'–3')	GGCCGACTTCACTGTACAACC
	Reverse (5'–3')	TCTGGGGTTCCTGGCACTTTG
NLRP3	Forward (5'–3')	GCTGCGATCAACAGGCGAGA
	Reverse (5'–3')	AAGGCTGTCCCTCCTGGCATAAC
ASC	Forward (5'–3')	CTGACGGATGAGCAGTACCA
	Reverse (5'–3')	CAGGATGATTTGGTGGGATT
Caspase-1	Forward (5'–3')	ACACGTCTTGCCCTCATTATCT
	Reverse (5'–3')	ATAACCTTGGGCTTGTCTTTCA
GSDMD-N	Forward (5'–3')	GGAGGAATTAATTGAGGCGGC
	Reverse (5'–3')	GGCACCAGTTCTCCAGAGTC
GSDME-N	Forward (5'–3')	CGTAGAGAGCCAGTCTTCATTT
	Reverse (5'–3')	GTTCCAGGACCATGAGTAGTTC

and electrotransferred onto polyvinylidene difluoride membranes (cat. ISEQ00010, Millipore, USA). The membranes were sequentially incubated with various primary antibodies and horseradish peroxidase-labeled secondary antibodies and finally subjected to chemiluminescent color development. The grayscale values of the bands of different sizes of proteins were analyzed using ImageJ software.

## ELISA

The activities of inflammatory factors, including TNF- $\alpha$ , IL-6, IL-18, and IL-1 $\beta$ , in BALF and lung tissues were detected via ELISA using the following kits according to the manufacturer's instructions: mouse IL-6 ELISA kits (Abcam, ab222503), mouse TNF- $\alpha$  ELISA kit (Abcam, ab208348), mouse IL-1 $\beta$  ELISA kits (Abcam, ab197742), and mouse IL-18 ELISA kit (Abcam, ab216165).

## Isolation of primary alveolar epithelial cells

Primary alveolar epithelial cells were isolated from lung tissues with different treatments using a previously described protocol [40]. Briefly, sterile PBS was instilled into the lungs of mice to drain all the remaining blood. The lungs were then digested with elastase (14 units/ml) and incubated at 37°C for 50 min. After incubation, the pulverized lung tissue was passed through a 20- $\mu$ m filter to prepare a dispersed single-cell

suspension. Fibroblasts and macrophages were removed by adhering them to a Petri dish coated with IgG. Isolated primary alveolar epithelial cells were confirmed via western blotting and immunofluorescence using antibodies targeting their cell-specific SP-C markers.

## Flow cytometry

Caspase-1 activity, an indicator of pyroptosis, was measured using the FLICA 660 Caspase-1 Assay kit (cat. 9122, ImmunoChemistry, USA). First, fetal bovine serum (FBS)-washed and trypsin-digested cells were resuspended in PBS with 2% FBS. Then, 660-YVAD-FMK was added to the cells as a fluorescent inhibitor probe that can label the active caspase-1 enzyme. The proportion of pyroptotic cells was measured using flow cytometry according to the manufacturer's instructions. BD FACSAria™ II cell sorter (BD Biosciences, USA) was used to analyze the data.

## Detection of H<sub>2</sub>S levels in lung tissues

Lung tissue homogenates were prepared in 100 mM of cold potassium phosphate buffer supplemented with protease inhibitors. Then, 100  $\mu$ l of homogenate and 1.2 M HCl containing 200  $\mu$ l of 30 mM ferric chloride (FeCl<sub>3</sub>) and 7.2 M HCl (containing 100  $\mu$ l of 1% zinc acetate, 100  $\mu$ l of borate buffer (pH = 10), and 200  $\mu$ l of 20 mM N,N-dimethyl-p-phenylenediamine dihydrochloride) was mixed and incubated in the dark

at 37°C for 15 min. Next, the sample was centrifuged at 4°C and 10000 rpm for 5 min. Subsequently, the supernatants were collected and the OD value was measured at 670 nm using a microplate reader (FilterMax F5, Molecular Devices). Finally, the H<sub>2</sub>S concentration was calculated according to the standard curve of sodium bisulfite solution [36].

### Statistical analysis

All data are presented as the means ± standard deviation. Results were analyzed using GraphPad Prism 8 software. Parameters were compared between two groups using a two-tailed Student's *t*-test. Differences at *p*-values of < 0.05 were considered statistically significant.

## RESULTS

### GO attenuates LPS-induced ALI

To investigate the effect of GO on ALI, we used a mouse model of LPS-induced ALI and administered GO at a dose of 100 mg/kg (Figure 1A). Histopathological features and scores indicative of the extent of lung injury in the LPS-induced ALI model are shown in Figure 1B, 1C. Compared to control mice, the lung tissue receiving LPS injections showed significant pathological changes, including interstitial lung edema, substantial infiltration of inflammatory cells, and hemorrhage in intra-alveolar and thickened interalveolar septa, indicating the presence of ALI. However, 100 mg/kg of GO pretreatment improved lung structure and inflammatory cell infiltration and significantly reduced lung injury scores (Figure 1B, 1C). However, no inhibitory effect of GO pretreatment on LPS-induced elevation of lung W/D ratio was observed (Figure 1D). Additionally, GO pretreatment remarkably reduced the level of MPO, an indicator of neutrophil infiltration, in the lungs, which was substantially elevated in LPS-induced ALI (Figure 1E). These results indicate that GO has a protective effect on LPS-induced lung injury.

BALF is also an important indicator of the severity of LPS-induced ALI and whether or not GO is protective. The degree of inflammatory cell infiltration into the alveoli was measured by staining cells collected from BALF. LPS significantly increased the number of cells in BALF, whereas GO pretreatment remarkably reduced the number of cells (Figure 1F, 1G). Furthermore, the total protein level inside BALF, as an indicator of pulmonary edema occurrence, can be used to evaluate pulmonary capillary permeability. As expected, compared with the control, the total protein level in BALF was much higher in the LPS group.

However, GO pretreatment reversed the LPS-induced increase in the total protein level in BALF, indicating that GO prevented the LPS-induced increase in capillary permeability (Figure 1H).

### GO blocks lung inflammation during LPS-induced ALI

Dysregulation of the systemic inflammatory response during infection is an important feature of ALI development [41]. The levels of inflammatory factors TNF- $\alpha$ , IL-6, IL-1 $\beta$  and IL-18 in ALI-infected lungs were detected via real-time PCR (Figure 2A) and western blotting (Figure 2B, 2C). The mRNA and protein levels of the aforementioned inflammatory cytokines demonstrated significant upregulation in the lungs that developed ALI after LPS treatment but were partially reduced by GO pretreatment (Figure 2A–2C). BALF was collected to measure systemic inflammation through ELISA, and the results showed that the levels of the aforementioned inflammatory cytokines in the BALF of ALI mice were also remarkably reduced by GO pretreatment (Figure 2D–2G). The findings reveal the vital anti-inflammatory effect of GO on ALI.

### GO inhibits the activation of NF- $\kappa$ B p65 and NLRP3-dependent inflammasome in LPS-induced ALI

The production of mature forms of IL-1 $\beta$  and IL-18 depends on NLRP3 inflammasome activation, which is potentially responsible for ALI development [42]. The marked activation of the NF- $\kappa$ B signaling pathway, which is involved in the transcriptional regulation of NLRP3 inflammasome activation and in the production of IL-6, TNF- $\alpha$ , pro-IL-1 $\beta$ , and pro-IL-18, is also closely related to LPS-induced ALI [43]. To further elucidate the mechanisms underlying the suppressive effects of GO on inflammatory cytokines, such as TNF- $\alpha$ , IL-6, IL-1 $\beta$ , and IL-18, in lungs with ALI, we further investigated the effect of GO on the expression of NF- $\kappa$ B and NLRP3 inflammasome pathway-related proteins. The western blotting results revealed significantly elevated protein expression levels of p-p65/p65 in the ALI group compared with the control group. However, GO pretreatment markedly reduced the expression of p-p65/p65 (Figure 3A, 3B). Additionally, we found that gene and protein expression levels of NLRP3, ASC, and cleaved caspase-1, which are the components that make up the inflammatory complex, were elevated in ALI lungs compared with controls and that GO pretreatment also reduced this expression (Figure 3C–3E). These results suggest that GO prevents endotoxemia-associated lung inflammation by mediating NF- $\kappa$ B phosphorylation and NLRP3/ASC/caspase-1 activation.

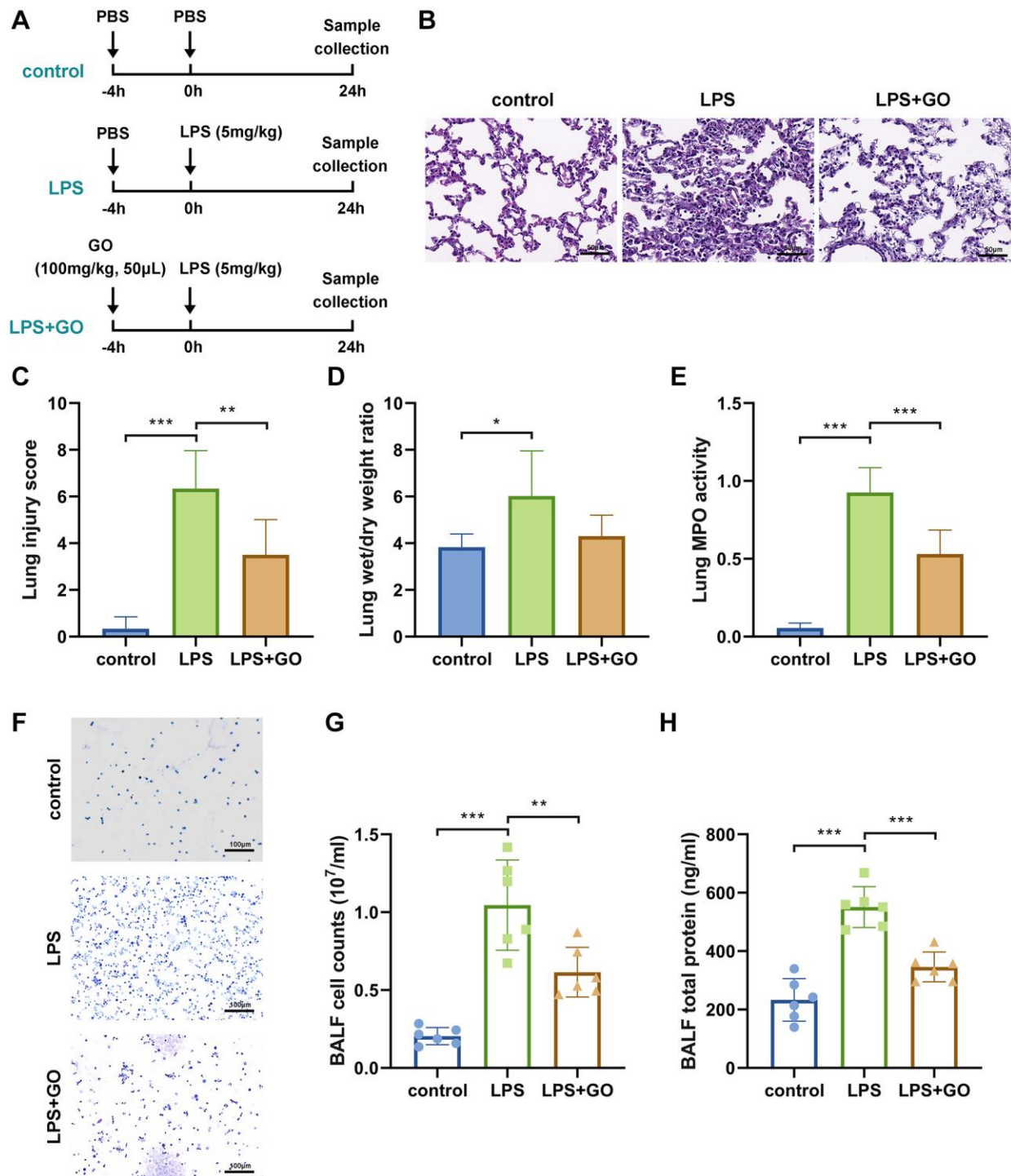


**Figure 1. GO attenuates LPS-induced ALI.** For ALI model establishment, mice were anesthetized via intraperitoneal injection of pentobarbital sodium (50 mg/kg) and then injected intratracheally with LPS (5 mg/kg) dissolved in 50  $\mu$ l PBS. Control mice were injected with the same volume of PBS. For GO delivery, mice were injected intratracheally with GO (100 mg/kg, dissolved in 50  $\mu$ l of DMSO) 4 h before LPS instillation. Samples (lung tissues and BALF) were collected 24 h after LPS instillation. (A) Flow chart of mouse experimental design. (B) Lung tissue sections stained with hematoxylin and eosin (H&E staining, scale bar: 50  $\mu$ m). (C) Severity of lung damage was scored on a scale of 0–10 according to inflammatory cell infiltration, alveolar septal edema and thickening, hyaline membrane formation, and pulmonary hemorrhage ( $n = 8$  per group). (D) Effect of GO on lung wet/dry ratio. (E) Quantification of MPO activity in lung tissue. (F) Cells were precipitated via BALF centrifugation and stained with Wright-Giemsa. (G) Cell counts in BALF samples from mice subjected to different treatments. (H) Total protein measurement in BALF via BCA assay. Experiments were performed in triplicate, and data are expressed as the mean  $\pm$  standard deviation (SD). Student's *t*-test; \* $p < 0.05$ , \*\* $p < 0.01$ , and \*\*\* $p < 0.001$  defined. Abbreviation: ns: no significant difference.

## GO blocks the expression of inflammatory pyroptosis-related proteins in LPS-induced ALI

Both the activation of the NLRP3/ASC/caspase-1 inflammasome complex and the substantial release of inflammatory cytokines, especially IL-1 $\beta$  and IL-18, in damaged lungs indicated that LPS-induced ALI may be associated with inflammatory pyroptosis. Hence, we conducted real-time PCR and western blotting to measure the expression levels of recognized pyroptosis marker proteins in the lung, the gasdermin family (GSDME and GSDMD). The active form of gasdermins

was significantly upregulated in LPS-induced ALI, which was effectively reversed by GO pretreatment (Figure 4A–4C). Subsequently, we investigated the pyroptosis ratio of primary alveolar epithelial cells via flow cytometry using propidium iodide and FLICA660 YVAD double staining. The proportion of pyroptotic cells was remarkably increased in LPS-induced ALI (from 2.12% to 9.06%) compared with control cells but was further reduced in GO-pretreated cells (from 9.06% to 5.15%) (Figure 4D, 4E). Collectively, these findings indicate that GO may alleviate LPS-induced ALI by blocking inflammation-related pyroptosis.

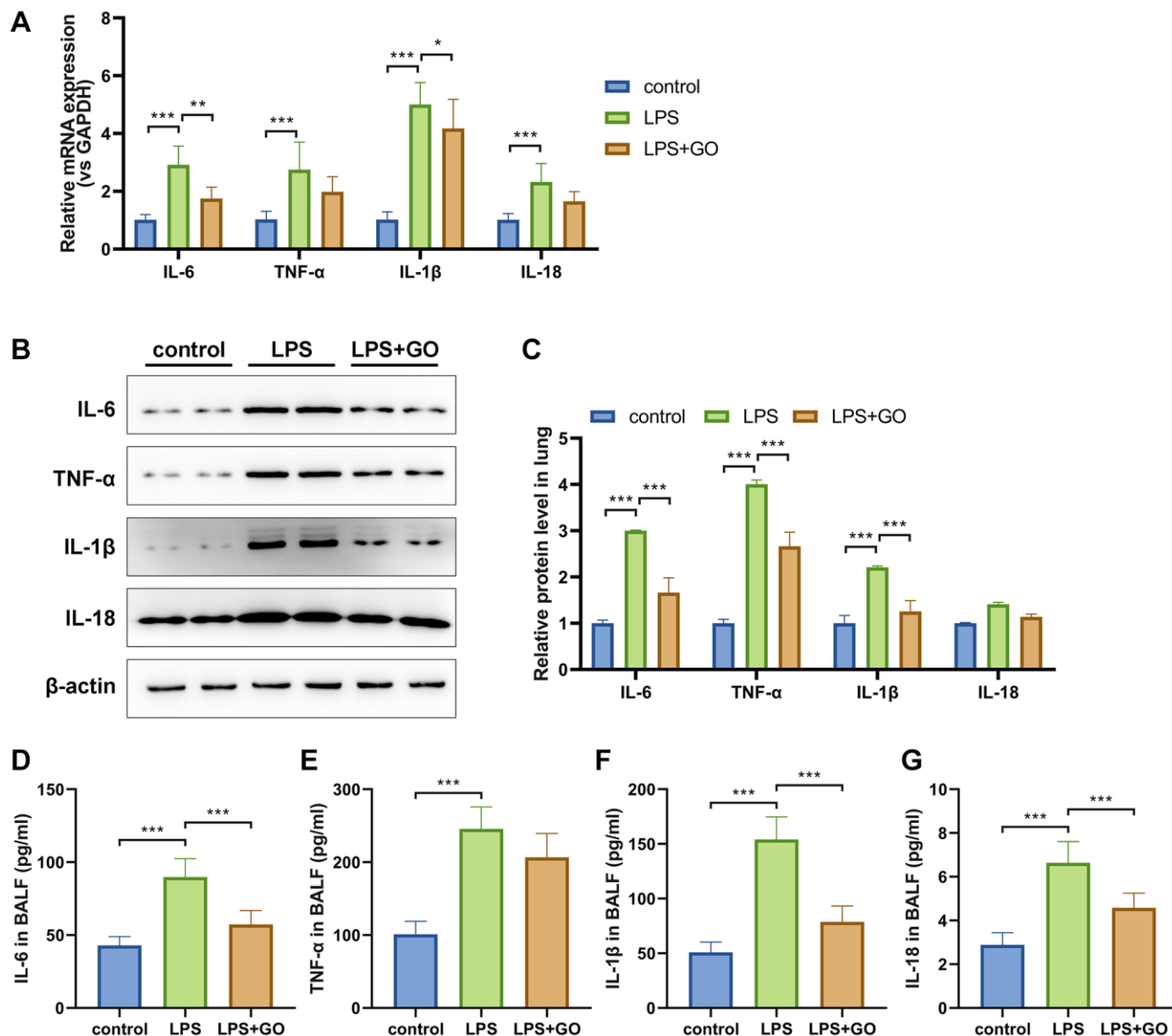


**Figure 2. GO blocks lung inflammation during LPS-induced ALI.** (A) Real-time PCR analysis showed that GO prevented the increase in the mRNA expression levels of inflammatory cytokines, including TNF- $\alpha$ , IL-6, IL-1 $\beta$ , and IL-18, in lung tissues. (B) Western blotting revealed that GO blocked the increase in the protein expression levels of inflammatory cytokines, including TNF- $\alpha$ , IL-6, IL-1 $\beta$ , and IL-18, in lung tissues. (C) Statistical chart of density analysis using ImageJ. (D–G) ELISA analysis revealed that GO inhibited the secretion of inflammation cytokines, including TNF- $\alpha$ , IL-6, IL-1 $\beta$ , and IL-18, in BALF. Experiments were performed in triplicate, and data are expressed as the mean  $\pm$  standard deviation (SD). Student's *t*-test, \**p* < 0.05, \*\**p* < 0.01, and \*\*\**p* < 0.001. Abbreviation: ns: no significant difference.

### GO attenuates LPS-induced ALI via H<sub>2</sub>S generation

Garlic is rich in polysulfide compounds, including DATS and diallyl disulfide, which liberate H<sub>2</sub>S *in vitro*. Additionally, GO therapy significantly increases the expression of H<sub>2</sub>S-producing enzymes, including CBS, CSE, and 3MST, in renal tissue [32]. H<sub>2</sub>S

reduces pyroptosis and alleviates acute kidney or lung injury by suppressing the NLRP3 inflammasome [36, 44]. Therefore, we further investigated whether the protective effects of GO on LPS-induced ALI were due to the release of H<sub>2</sub>S. First, we detected the effects of GO on the expression of three H<sub>2</sub>S-producing enzymes, including CBS, CSE, and 3MST, in lung tissue via

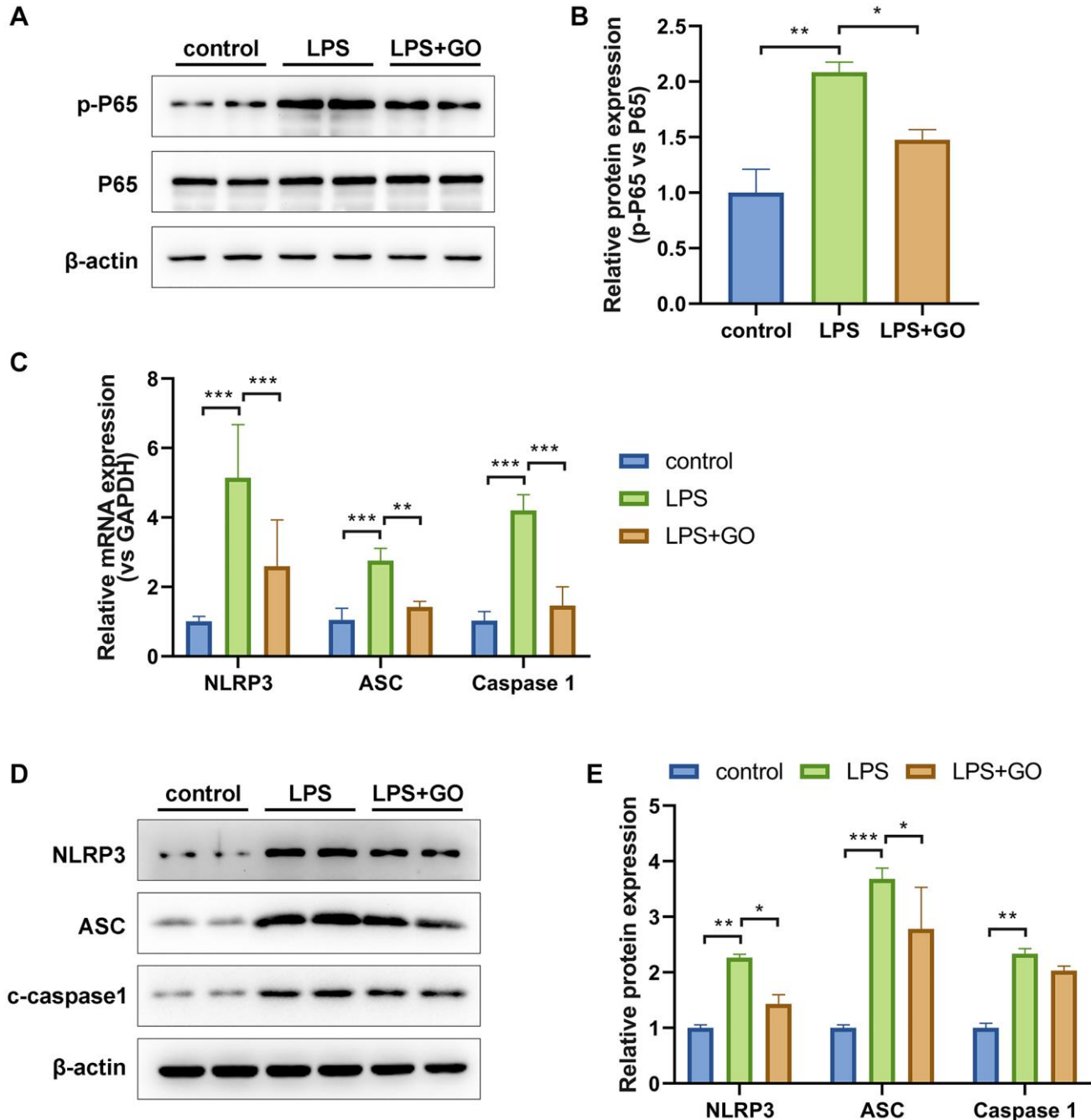


**Figure 3. GO inhibits the activation of NF-κB p65 and NLRP3 inflammasome in LPS-induced ALI.** (A) Western blot analysis of phosphorylated NF-κB p65 levels in lung tissue. (B) The grayscale values of the bands in image A were analyzed using ImageJ, and the ratios of p-p65/p65 were calculated. (C) Real-time PCR analysis of mRNA expression levels of the NLRP3/ASC/caspase 1 inflammasome complex in lung tissue. (D) Western blotting analysis of protein expression levels of the NLRP3/ASC/caspase 1 inflammasome complex in lung tissue. (E) A histogram of the grayscale values of the protein bands calculated using ImageJ software (standardized to β-actin). Experiments were performed in triplicate. Student's *t*-test, \**p* < 0.05, \*\**p* < 0.01, and \*\*\**p* < 0.001. Abbreviation: ns: no significant difference.

western blotting. The results revealed that the LPS-treated group displayed a slight increase in the expression levels of CBS and CSE compared with the controls, whereas a remarkable increase in the expression levels of CBS and CSE was observed in the GO pretreatment group. However, the expression levels of 3MST did not differ among the three groups (Figure 5A, 5B). Consistent with the above results, we found that LPS treatment slightly increased H<sub>2</sub>S production, whereas GO pretreatment substantially increased H<sub>2</sub>S production in lung tissue compared with the control group (Figure 5C).

Based on our observation that GO treatment significantly increases H<sub>2</sub>S production, we hypothesized that the protective effects of GO in LPS-induced ALI are associated with H<sub>2</sub>S production. To confirm this hypothesis, we continued to investigate whether the removal of H<sub>2</sub>S could reverse the protective effect of GO. H<sub>2</sub>S in the lungs can be converted by polysulfide compounds in garlic, such as DATS (exogenously produced H<sub>2</sub>S) or can be produced *in vivo* by H<sub>2</sub>S-producing enzymes (endogenously produced H<sub>2</sub>S). Therefore, IAM (an effective inhibitor of the conversion

of DATS to H<sub>2</sub>S *in vivo*) was used to remove exogenous H<sub>2</sub>S, and AOAA (CBS inhibitor) and PAG (CSE inhibitor) were used to remove endogenous H<sub>2</sub>S (Figure 5D). The lung histological pathology revealed that GO pretreatment significantly improved LPS-induced lung injury, whereas cotreatment with IAM or AOAA and PAG reversed the protective effects of GO on ALI and increased the lung injury scores again (Figure 5E, 5F). The results from cell counts in BALF revealed a similar trend (Figure 5G). These results indicate that GO attenuated LPS-induced ALI via the H<sub>2</sub>S-generating pathway.

### GO inhibits NF-κB and NLRP3 inflammasome-mediated inflammatory pyroptosis in LPS-induced ALI via H<sub>2</sub>S generation

Next, we explored whether the potential mechanism underlying the suppressive effects of GO on NF-κB and NLRP3 inflammasome-associated inflammatory pyroptosis was related to the production of H<sub>2</sub>S. First, we measured the levels of the inflammatory cytokines TNF-α, IL-6, IL-1β, and IL-18 in the lungs and BALF of ALI mice in different groups via ELISA. The results

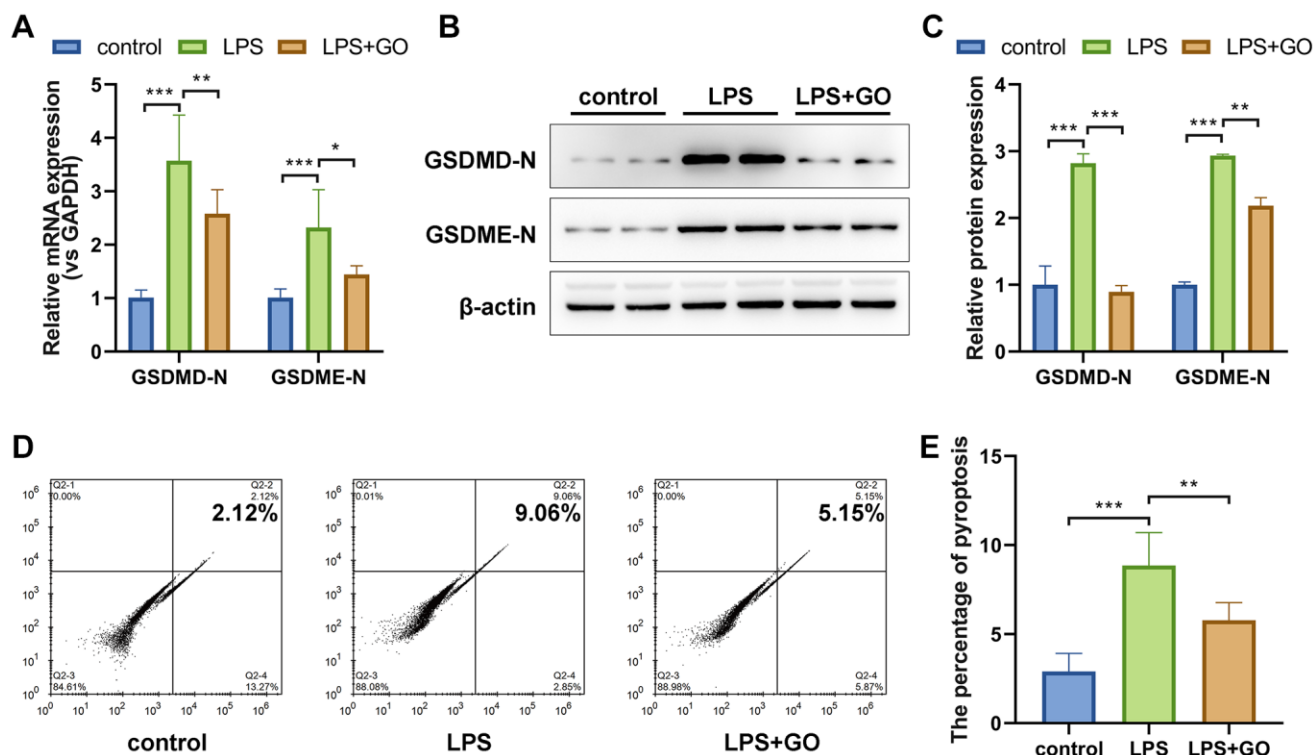


**Figure 4. GO blocks the expression of pyroptosis-related proteins in LPS-induced ALI.** (A) mRNA expression levels of the active forms of the pyroptosis-related proteins GSDMD and GSDME in lung tissue were analyzed via real-time PCR. (B) Protein expression levels of the active forms of the pyroptosis-related proteins GSDMD and GSDME in lung tissue were analyzed via western blotting. (C) A histogram of the grayscale values of the protein bands calculated using ImageJ software (standardized to β-actin). (D) The pyroptosis rate of isolated primary alveolar epithelial cells was analyzed using flow cytometry and FLICA caspase-1 and PI double staining. (E) The incident rate of pyroptosis was calculated for each group. Experiments were performed in triplicate, and data are expressed as the mean ± standard deviation (SD). Student's *t*-test, \**p* < 0.05, \*\**p* < 0.01, and \*\*\**p* < 0.001. Abbreviation: ns: no significant difference.

revealed that GO inhibited the expression of inflammatory cytokines in the lungs and BALF in LPS-induced ALI. However, the inhibitory effects of GO on

inflammatory cytokine expression were significantly attenuated upon treatment with IAM or a combination of AOAA and PAG (Figure 6A–6H). Additionally, we

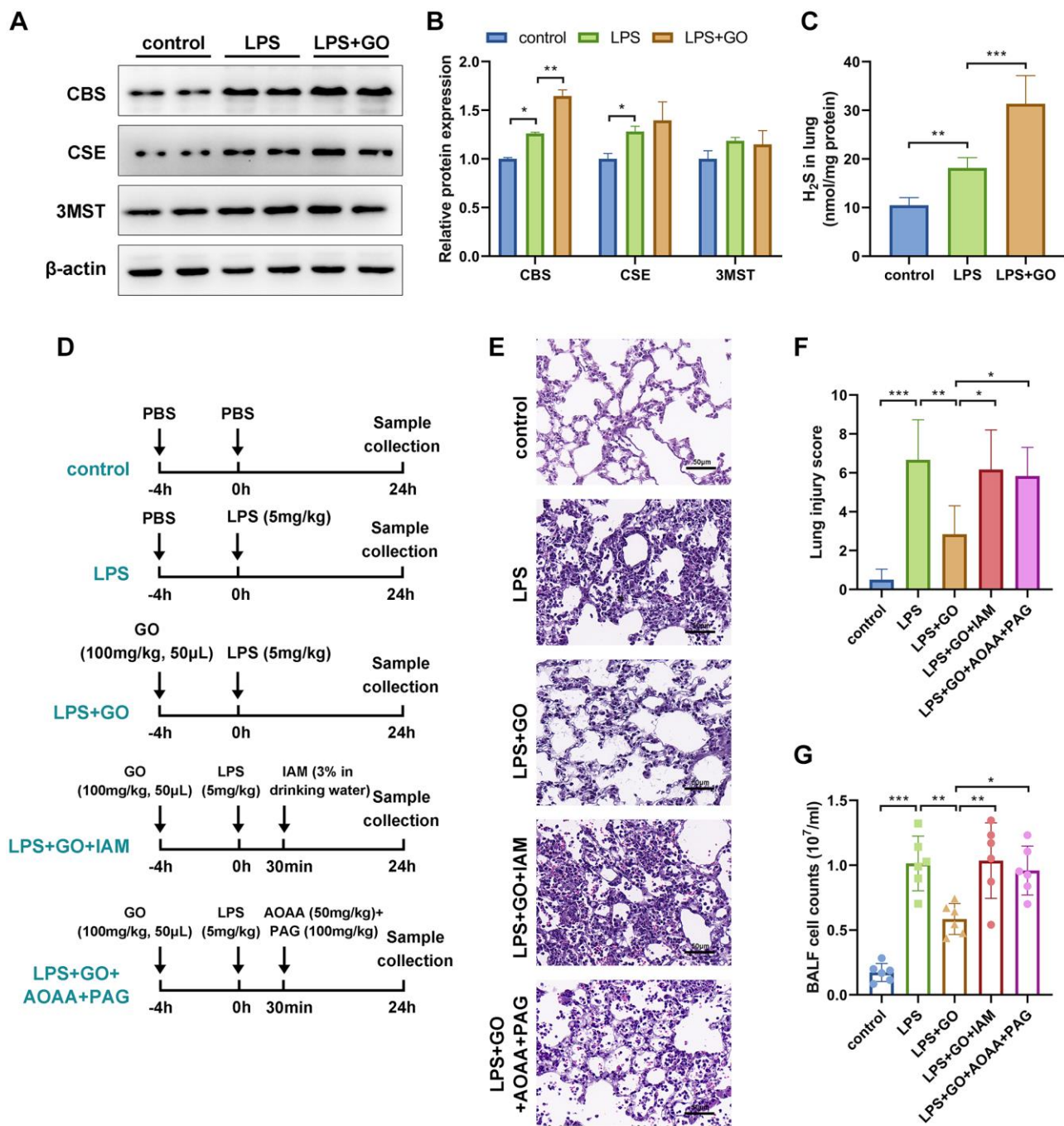


**Figure 5. GO alleviated LPS-induced ALI via the H<sub>2</sub>S generating pathway.** (A) Western blotting to detect the protein expression levels of three H<sub>2</sub>S-producing enzymes, namely CBS, CSE, and 3MST, in lung tissue. (B) The grayscale values of the bands in image A were normalized to β-actin and analyzed using ImageJ software. (C) Detection of H<sub>2</sub>S levels in lung tissues. (D) Flow diagrams of mice experiments. IAM is an effective inhibitor of the conversion of DATS to H<sub>2</sub>S *in vivo*. For IAM delivery, mice were administered 3% IAM in their drinking water 30 min after LPS instillation. AOAA is a CBS inhibitor and PAG is a CSE inhibitor. For AOAA and PAG delivery, mice were intraperitoneally injected with AOAA (50 mg/kg) and PAG (100 mg/kg), respectively, 30 min after LPS instillation. (E) Lung tissue sections stained with hematoxylin and eosin (H&E staining, scale bar: 50 μm). (F) Severity of lung damage was scored on a scale of 0–10 according to inflammatory cell infiltration, alveolar septal edema and thickening, hyaline membrane formation, and pulmonary hemorrhage (*n* = 8 per group). (G) The total number of cells exuded in BALF. Data are expressed as the mean ± SD. Student's *t*-test, \**p* < 0.05, \*\**p* < 0.01, and defined as \*\*\**p* < 0.001. Abbreviation: ns: no significant difference.

observed that GO effectively inhibited the expression of p-p65/p65, NLRP3, ASC, cleaved caspase-1, GSDMD-N, and GSDME-N in LPS-induced ALI. However, when cotreated with IAM or AOAA and

PAG to remove exogenous or endogenous H<sub>2</sub>S, the inhibitory effects of GO on the activation of NF- $\kappa$ B, NLRP3 inflammasome complex, and pyroptosis in LPS-induced ALI were significantly weakened (Figure 6I, 6J).

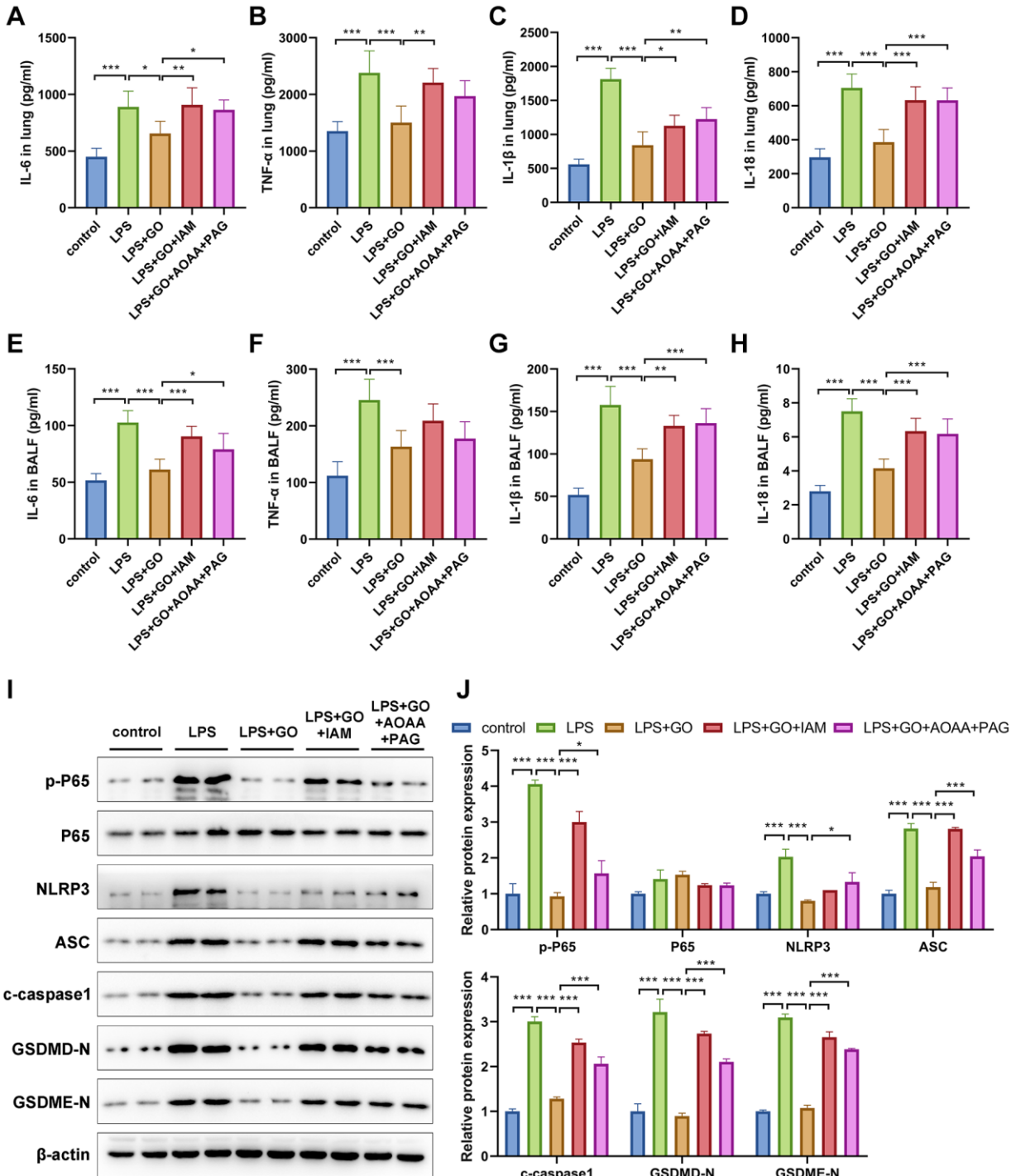


**Figure 6. GO inhibits the NF- $\kappa$ B signaling and NLRP3 inflammasome-mediated inflammatory pyroptosis in LPS-induced ALI via the H<sub>2</sub>S-generating pathway.** (A–D) ELISA of the levels of inflammatory cytokines, including TNF- $\alpha$ , IL-6, IL-1 $\beta$ , and IL-18, in lungs. (E–H) ELISA of the levels of secreted inflammatory cytokines, including TNF- $\alpha$ , IL-6, IL-1 $\beta$ , and IL-18, in BALF. (I) Western blotting to detect the protein expression levels of p-p65, p65, NLRP3, ASC, c-caspase 1, and apoptotic markers in lungs. (J) The grayscale values of the bands in the image were normalized to  $\beta$ -actin and analyzed using ImageJ software. Data are expressed as the means  $\pm$  SD. Student's *t*-test, \**p* < 0.05, \*\**p* < 0.01, and \*\*\**p* < 0.001. Abbreviation: ns: no significant difference.

Accordingly, we propose that GO inhibited NF- $\kappa$ B and NLRP3 inflammasome-mediated inflammatory pyroptosis in LPS-induced ALI and that this phenomenon was partially associated with the H<sub>2</sub>S-generating pathway.

## DISCUSSION

ALI is a significant contributor to critical acute respiratory failure [45]. To date, therapeutic strategies specific to ALI remain limited. With the continuous development of modern medicine, many active ingredients from plants or food with antimicrobial, anti-inflammatory, and antioxidant activities have been identified to exhibit some degree of efficacy in preventing and treating ALIs [18, 19]. Garlic, a globally used cooking spice, has numerous medicinal effects. It has anti-inflammatory, immunomodulatory, and metabolic regulatory properties, playing a preventive and protective role in various degenerative illnesses, such as hyperlipidemia, cardiovascular disease, and cancer [20, 21, 32, 46]. This study aimed to explore the therapeutic effect of GO on LPS-induced ALI. Rewardingly, we discovered that GO pretreatment significantly inhibited LPS-induced ALI, including improving lung pathology, reducing the lung W/D ratio, and decreasing inflammatory cell counts and protein levels in BALF samples.

To date, the pathogenesis of ALI remains unclear. Immunomodulatory and inflammatory processes play a non-negligible role in the progression of multifactorial-promoted ALIs [47]. Inflammation, in particular, is recognized as a major contributor to lung injury [48]. An inflammatory response consisting of a complex network of cytokines has been found to be a major feature of LPS-induced ALI [49]. Hence, we explored the function of GO in regulating inflammatory responses in LPS-induced ALI. Consistent with the above study, we found elevated levels of inflammatory cytokines, such as TNF- $\alpha$ , IL-6, IL-1 $\beta$ , and IL-18, in the lungs and BALF samples of mice with LPS-induced ALI. However, the upregulation of inflammatory cytokine levels in the lungs and BALF samples in ALI was prevented by GO pretreatment. Additionally, studies have revealed that the severity of ALI may be exacerbated if pulmonary neutrophil infiltration occurs during the early stages of the inflammatory processes of ALI [50–52]. The activity of MPO, an enzyme contained within neutrophils, is a useful indicator of pulmonary infiltration of neutrophils. In this study, we also found that the LPS-induced upregulation of MPO activity was significantly inhibited by GO. These results strongly indicate that GO effectively protected the lung from LPS-induced inflammation injury.

Among the various inflammatory pathways, the NF- $\kappa$ B pathway and NLRP3 inflammasome are the primary molecular pathways. NF- $\kappa$ B has been reported as a key signaling molecule with an important role in regulating inflammatory mediators [53]. NF- $\kappa$ B overresponse worsens lung inflammation [43]. The NLRP3 inflammasome, which is activated by the assembly of the three components NLRP3, ASC, and caspase-1 into a protein complex, is a prerequisite for the maturation and release of IL-1 $\beta$  and IL-18 [54]. Suppression of NLRP3 activation alleviates LPS-induced ALI [13]. We explored GO regulation of inflammation by targeting the NF- $\kappa$ B pathway and NLRP3 inflammasome. Our results revealed that GO remarkably inhibited the LPS-induced activation of NF- $\kappa$ B and NLRP3 inflammasome. Pyroptosis is an emerging form of inflammatory cell death that frequently occurs during the pathogenesis of inflammation, and the NLRP3 inflammasome contributes to the induction of pyroptosis in LPS-induced ALI [55]. In the present study, we confirmed that pyroptosis occurred and that the levels of pyroptosis markers, such as GSDMD and GSDME, were elevated in LPS-induced ALI but were reduced by GO pretreatment. Our data suggested that GO inhibited LPS-induced ALI by suppressing the NF- $\kappa$ B pathway and NLRP3 inflammasome as well as inflammatory-related pyroptosis.

Many organic polysulfides, such as DATS and diallyl disulfide, are present in GO and release H<sub>2</sub>S under physiological conditions. Thus, GO is an exogenous H<sub>2</sub>S donor. Additionally, other studies and our experimental results both demonstrated that GO could significantly increase the expression level of H<sub>2</sub>S-producing enzymes *in vivo*, thereby increasing the production of endogenous H<sub>2</sub>S [32]. Recently, an increasing number of studies have revealed that H<sub>2</sub>S is not only a toxic gas molecule but also has many beneficial physiological effects, such as antiapoptosis, antioxidation, and anti-inflammation. H<sub>2</sub>S can also prevent acute endotoxemia-induced lung injury [28, 29]. Accordingly, we aimed to explore whether the protective effect of GO on LPS-induced ALI was due to the H<sub>2</sub>S-generating pathway. We found that the protective effects of GO on ALI as well as the inhibitory effects of GO on the NF- $\kappa$ B pathway, NLRP3 inflammasome, and inflammatory pyroptosis were reversed when endogenous and exogenous H<sub>2</sub>S were removed. Our findings indicated that H<sub>2</sub>S production may be the major mechanism underlying the protective effect of GO on LPS-induced ALI.

In conclusion, our findings suggested that GO had a protective effect on LPS-induced ALI in mice via the suppression of the inflammatory response.

The inhibitory effects were due to the inhibition of NF- $\kappa$ B, NLRP3, and the inflammatory pyroptotic pathway. GO exerts these effects by regulating the H<sub>2</sub>S-generating pathway. In summary, our study demonstrates that the application of GO helps prevent LPS-induced ALI. In a future study, positive control and biosafety analyses will be performed to further explore the clinical potential of GO.

## Abbreviations

ALI: Acute lung injury; ARDS: Acute respiratory distress syndrome; GO: Garlic oil; LPS: Lipopolysaccharide; GSDMD: Gasdermin D; GSDME: Gasdermin E; DATS: Diallyl trisulfide; CBS: Cystathionine  $\beta$ -synthase; CSE: Cystathionine  $\gamma$ -lyase; 3MST: 3-mercaptopyruvate sulphurtransferase; H<sub>2</sub>S: Hydrogen sulfide; IAM: Iodoacetamide; AOAA: Amino-oxyacetic acid; PAG: DL-propargylglycine; BALF: Bronchoalveolar lavage fluid; H&E: Hematoxylin–eosin; SDS-PAGE: Sodium dodecyl sulfate–polyacrylamide gel electrophoresis.

## AUTHOR CONTRIBUTIONS

Tursunay Dilxat designed the study. Tursunay Dilxat, Qiang Shi, Xiaofan Chen, and Xuxin Liu performed the experiments and analyzed the data. Xuxin Liu contributed to the new methods and wrote the paper.

## CONFLICTS OF INTEREST

The authors declare no conflicts of interest related to this study.

## ETHICAL STATEMENT

All trial animal procedures were approved by The Ethics Committee of Xinjiang Agricultural Vocational Technological College (approval number 2022 (01)).

## FUNDING

This study was supported by the 2022 Xinjiang Agricultural Extension and Service Project.

## REFERENCES

1. Bellani G, Laffey JG, Pham T, Fan E, Brochard L, Esteban A, Gattinoni L, van Haren F, Larsson A, McAuley DF, Ranieri M, Rubenfeld G, Thompson BT, et al, and LUNG SAFE Investigators, and ESICM Trials Group. Epidemiology, Patterns of Care, and Mortality for Patients With Acute Respiratory Distress Syndrome in Intensive Care Units in 50 Countries. *JAMA*. 2016; 315:788–800. <https://doi.org/10.1001/jama.2016.0291> PMID:26903337
2. Sweeney RM, McAuley DF. Acute respiratory distress syndrome. *Lancet*. 2016; 388:2416–30. [https://doi.org/10.1016/S0140-6736\(16\)00578-X](https://doi.org/10.1016/S0140-6736(16)00578-X) PMID:27133972
3. Bhattacharya J, Matthay MA. Regulation and repair of the alveolar-capillary barrier in acute lung injury. *Annu Rev Physiol*. 2013; 75:593–615. <https://doi.org/10.1146/annurev-physiol-030212-183756> PMID:23398155
4. Guerin C, Bayle F, Leray V, Debord S, Stoian A, Yonis H, Roudaut JB, Bourdin G, Devouassoux-Shisheboran M, Bucher E, Ayzac L, Lantuejoul S, Philipponnet C, et al. Open lung biopsy in nonresolving ARDS frequently identifies diffuse alveolar damage regardless of the severity stage and may have implications for patient management. *Intensive Care Med*. 2015; 41:222–30. <https://doi.org/10.1007/s00134-014-3583-2> PMID:25476984
5. An X, Sun X, Hou Y, Yang X, Chen H, Zhang P, Wu J. Protective effect of oxytocin on LPS-induced acute lung injury in mice. *Sci Rep*. 2019; 9:2836. <https://doi.org/10.1038/s41598-019-39349-1> PMID:30808956
6. Hu X, Tian Y, Qu S, Cao Y, Li S, Zhang W, Zhang Z, Zhang N, Fu Y. Protective effect of TM6 on LPS-induced acute lung injury in mice. *Sci Rep*. 2017; 7:572. <https://doi.org/10.1038/s41598-017-00551-8> PMID:28373694
7. Butt Y, Kurdowska A, Allen TC. Acute Lung Injury: A Clinical and Molecular Review. *Arch Pathol Lab Med*. 2016; 140:345–50. <https://doi.org/10.5858/arpa.2015-0519-RA> PMID:27028393
8. Shen W, Gan J, Xu S, Jiang G, Wu H. Penehyclidine hydrochloride attenuates LPS-induced acute lung injury involvement of NF-kappaB pathway. *Pharmacol Res*. 2009; 60:296–302. <https://doi.org/10.1016/j.phrs.2009.04.007> PMID:19386282
9. Liu S, Feng G, Wang GL, Liu GJ. p38MAPK inhibition attenuates LPS-induced acute lung injury involvement of NF-kappaB pathway. *Eur J Pharmacol*. 2008; 584:159–65. <https://doi.org/10.1016/j.ejphar.2008.02.009> PMID:18328478
10. Wang B, Gong X, Wan JY, Zhang L, Zhang Z, Li HZ, Min S. Resolvin D1 protects mice from LPS-induced acute lung injury. *Pulm Pharmacol Ther*. 2011; 24:434–41.

<https://doi.org/10.1016/j.pupt.2011.04.001>

PMID:[21501693](https://pubmed.ncbi.nlm.nih.gov/21501693/)

11. Everhart MB, Han W, Sherrill TP, Arutiunov M, Polosukhin VV, Burke JR, Sadikot RT, Christman JW, Yull FE, Blackwell TS. Duration and intensity of NF-kappaB activity determine the severity of endotoxin-induced acute lung injury. *J Immunol*. 2006; 176:4995–5005.  
<https://doi.org/10.4049/jimmunol.176.8.4995>  
PMID:[16585596](https://pubmed.ncbi.nlm.nih.gov/16585596/)
12. Liu B, Wu Y, Wang Y, Cheng Y, Yao L, Liu Y, Qian H, Yang H, Shen F. NF-κB p65 Knock-down inhibits TF, PAI-1 and promotes activated protein C production in lipopolysaccharide-stimulated alveolar epithelial cells type II. *Exp Lung Res*. 2018; 44:241–51.  
<https://doi.org/10.1080/01902148.2018.1505975>  
PMID:[30449218](https://pubmed.ncbi.nlm.nih.gov/30449218/)
13. Zhang Y, Li X, Graier JJ, Wang N, Wang M, Yao J, Zhong R, Gao GF, Ward PA, Tan DX, Li X. Melatonin alleviates acute lung injury through inhibiting the NLRP3 inflammasome. *J Pineal Res*. 2016; 60:405–14.  
<https://doi.org/10.1111/jpi.12322>  
PMID:[26888116](https://pubmed.ncbi.nlm.nih.gov/26888116/)
14. Shi J, Gao W, Shao F. Pyroptosis: Gasdermin-Mediated Programmed Necrotic Cell Death. *Trends Biochem Sci*. 2017; 42:245–54.  
<https://doi.org/10.1016/j.tibs.2016.10.004>  
PMID:[27932073](https://pubmed.ncbi.nlm.nih.gov/27932073/)
15. Aglietti RA, Dueber EC. Recent Insights into the Molecular Mechanisms Underlying Pyroptosis and Gasdermin Family Functions. *Trends Immunol*. 2017; 38:261–71.  
<https://doi.org/10.1016/j.it.2017.01.003>  
PMID:[28196749](https://pubmed.ncbi.nlm.nih.gov/28196749/)
16. Hou L, Yang Z, Wang Z, Zhang X, Zhao Y, Yang H, Zheng B, Tian W, Wang S, He Z, Wang X. NLRP3/ASC-mediated alveolar macrophage pyroptosis enhances HMGB1 secretion in acute lung injury induced by cardiopulmonary bypass. *Lab Invest*. 2018; 98:1052–64.  
<https://doi.org/10.1038/s41374-018-0073-0>  
PMID:[29884910](https://pubmed.ncbi.nlm.nih.gov/29884910/)
17. Pinkerton JW, Kim RY, Robertson AAB, Hirota JA, Wood LG, Knight DA, Cooper MA, O'Neill LAJ, Horvat JC, Hansbro PM. Inflammasomes in the lung. *Mol Immunol*. 2017; 86:44–55.  
<https://doi.org/10.1016/j.molimm.2017.01.014>  
PMID:[28129896](https://pubmed.ncbi.nlm.nih.gov/28129896/)
18. Mahalanobish S, Saha S, Dutta S, Sil PC. Corrigendum on "Mangiferin alleviates arsenic induced oxidative lung injury via upregulation of the Nrf2-HO1 axis" [126 (2019) 41-55]. *Food Chem Toxicol*. 2023; 182:114194.  
<https://doi.org/10.1016/j.fct.2023.114194>  
PMID:[38000267](https://pubmed.ncbi.nlm.nih.gov/38000267/)
19. Dong ZW, Yuan YF. Juglanin suppresses fibrosis and inflammation response caused by LPS in acute lung injury. *Int J Mol Med*. 2018; 41:3353–65.  
<https://doi.org/10.3892/ijmm.2018.3554>  
PMID:[29532887](https://pubmed.ncbi.nlm.nih.gov/29532887/)
20. Zhang Y, Liu X, Ruan J, Zhuang X, Zhang X, Li Z. Phytochemicals of garlic: Promising candidates for cancer therapy. *Biomed Pharmacother*. 2020; 123:109730.  
<https://doi.org/10.1016/j.biopha.2019.109730>  
PMID:[31877551](https://pubmed.ncbi.nlm.nih.gov/31877551/)
21. Sobenin IA, Myasoedova VA, Iltchuk MI, Zhang DW, Orekhov AN. Therapeutic effects of garlic in cardiovascular atherosclerotic disease. *Chin J Nat Med*. 2019; 17:721–8.  
[https://doi.org/10.1016/S1875-5364\(19\)30088-3](https://doi.org/10.1016/S1875-5364(19)30088-3)  
PMID:[31703752](https://pubmed.ncbi.nlm.nih.gov/31703752/)
22. Quesada I, de Paola M, Torres-Palazzolo C, Camargo A, Ferder L, Manucha W, Castro C. Effect of Garlic's Active Constituents in Inflammation, Obesity and Cardiovascular Disease. *Curr Hypertens Rep*. 2020; 22:6.  
<https://doi.org/10.1007/s11906-019-1009-9>  
PMID:[31925548](https://pubmed.ncbi.nlm.nih.gov/31925548/)
23. Arreola R, Quintero-Fabián S, López-Roa RI, Flores-Gutiérrez EO, Reyes-Grajeda JP, Carrera-Quintanar L, Ortuño-Sahagún D. Immunomodulation and anti-inflammatory effects of garlic compounds. *J Immunol Res*. 2015; 2015:401630.  
<https://doi.org/10.1155/2015/401630>  
PMID:[25961060](https://pubmed.ncbi.nlm.nih.gov/25961060/)
24. Zhang CL, Zeng T, Zhao XL, Xie KQ. Garlic Oil Suppressed Nitrosodiethylamine-Induced Hepatocarcinoma in Rats by Inhibiting PI3K-AKT-NF-κB Pathway. *Int J Biol Sci*. 2015; 11:643–51.  
<https://doi.org/10.7150/ijbs.10785>  
PMID:[25999787](https://pubmed.ncbi.nlm.nih.gov/25999787/)
25. Amagase H, Petesch BL, Matsuura H, Kasuga S, Itakura Y. Intake of garlic and its bioactive components. *J Nutr*. 2001; 131:955S–62S.  
<https://doi.org/10.1093/jn/131.3.955S>  
PMID:[11238796](https://pubmed.ncbi.nlm.nih.gov/11238796/)
26. Shang A, Cao SY, Xu XY, Gan RY, Tang GY, Corke H, Mavumengwana V, Li HB. Bioactive Compounds and Biological Functions of Garlic (*Allium sativum* L.). *Foods*. 2019; 8:246.  
<https://doi.org/10.3390/foods8070246>  
PMID:[31284512](https://pubmed.ncbi.nlm.nih.gov/31284512/)
27. Lee DY, Li H, Lim HJ, Lee HJ, Jeon R, Ryu JH. Anti-inflammatory activity of sulfur-containing compounds from garlic. *J Med Food*. 2012; 15:992–9.

- <https://doi.org/10.1089/jmf.2012.2275>  
PMID:23057778
28. Li J, Li M, Li L, Ma J, Yao C, Yao S. Hydrogen sulfide attenuates ferroptosis and stimulates autophagy by blocking mTOR signaling in sepsis-induced acute lung injury. *Mol Immunol.* 2022; 141:318–27.  
<https://doi.org/10.1016/j.molimm.2021.12.003>  
PMID:34952420
29. Zhang HX, Liu SJ, Tang XL, Duan GL, Ni X, Zhu XY, Liu YJ, Wang CN. H<sub>2</sub>S Attenuates LPS-Induced Acute Lung Injury by Reducing Oxidative/Nitrative Stress and Inflammation. *Cell Physiol Biochem.* 2016; 40:1603–12.  
<https://doi.org/10.1159/000453210>  
PMID:28006762
30. Kimura H. The physiological role of hydrogen sulfide and beyond. *Nitric Oxide.* 2014; 41:4–10.  
<https://doi.org/10.1016/j.niox.2014.01.002>  
PMID:24491257
31. Hsu CN, Tain YL. Hydrogen Sulfide in Hypertension and Kidney Disease of Developmental Origins. *Int J Mol Sci.* 2018; 19:1438.  
<https://doi.org/10.3390/ijms19051438>  
PMID:29751631
32. Hsu CN, Hou CY, Chang-Chien GP, Lin S, Tain YL. Maternal Garlic Oil Supplementation Prevents High-Fat Diet-Induced Hypertension in Adult Rat Offspring: Implications of H<sub>2</sub>S-Generating Pathway in the Gut and Kidneys. *Mol Nutr Food Res.* 2021; 65:e2001116.  
<https://doi.org/10.1002/mnfr.202001116>  
PMID:33547712
33. Bazhanov N, Ansar M, Ivanciuc T, Garofalo RP, Casola A. Hydrogen Sulfide: A Novel Player in Airway Development, Pathophysiology of Respiratory Diseases, and Antiviral Defenses. *Am J Respir Cell Mol Biol.* 2017; 57:403–10.  
<https://doi.org/10.1165/rcmb.2017-0114TR>  
PMID:28481637
34. Han W, Dong Z, Dimitropoulou C, Su Y. Hydrogen sulfide ameliorates tobacco smoke-induced oxidative stress and emphysema in mice. *Antioxid Redox Signal.* 2011; 15:2121–34.  
<https://doi.org/10.1089/ars.2010.3821>  
PMID:21504365
35. Wang Z, Yin X, Gao L, Feng S, Song K, Li L, Lu Y, Shen H. The protective effect of hydrogen sulfide on systemic sclerosis associated skin and lung fibrosis in mice model. *Springerplus.* 2016; 5:1084.  
<https://doi.org/10.1186/s40064-016-2774-4>  
PMID:27468384
36. Ni J, Jiang L, Shen G, Xia Z, Zhang L, Xu J, Feng Q, Qu H, Xu F, Li X. Hydrogen sulfide reduces pyroptosis and alleviates ischemia-reperfusion-induced acute kidney injury by inhibiting NLRP3 inflammasome. *Life Sci.* 2021; 284:119466.  
<https://doi.org/10.1016/j.lfs.2021.119466>  
PMID:33811893
37. Lestari SR, Christina YI, Atho'llah MF, Rifa'i M. Single-bulb garlic oil regulates toll-like receptors and Nrf2 cross-talk and IL-17 production in mice fed with high-fat diet. *Saudi J Biol Sci.* 2021; 28:6515–22.  
<https://doi.org/10.1016/j.sjbs.2021.07.021>  
PMID:34764767
38. Zeng T, Zhang CL, Song FY, Han XY, Xie KQ. The modulatory effects of garlic oil on hepatic cytochrome P450s in mice. *Hum Exp Toxicol.* 2009; 28:777–83.  
<https://doi.org/10.1177/0960327109353057>  
PMID:19875617
39. Matute-Bello G, Downey G, Moore BB, Groshong SD, Matthay MA, Slutsky AS, Kuebler WM, and Acute Lung Injury in Animals Study Group. An official American Thoracic Society workshop report: features and measurements of experimental acute lung injury in animals. *Am J Respir Cell Mol Biol.* 2011; 44:725–38.  
<https://doi.org/10.1165/rcmb.2009-0210ST>  
PMID:21531958
40. Driscoll B, Kikuchi A, Lau AN, Lee J, Reddy R, Jesudason E, Kim CF, Warburton D. Isolation and characterization of distal lung progenitor cells. *Methods Mol Biol.* 2012; 879:109–22.  
[https://doi.org/10.1007/978-1-61779-815-3\\_7](https://doi.org/10.1007/978-1-61779-815-3_7)  
PMID:22610556
41. Matthay MA, Zemans RL, Zimmerman GA, Arabi YM, Beitler JR, Mercat A, Herridge M, Randolph AG, Calfee CS. Acute respiratory distress syndrome. *Nat Rev Dis Primers.* 2019; 5:18.  
<https://doi.org/10.1038/s41572-019-0069-0>  
PMID:30872586
42. Zhang T, Li M, Zhao S, Zhou M, Liao H, Wu H, Mo X, Wang H, Guo C, Zhang H, Yang N, Huang Y. CaMK4 Promotes Acute Lung Injury Through NLRP3 Inflammasome Activation in Type II Alveolar Epithelial Cell. *Front Immunol.* 2022; 13:890710.  
<https://doi.org/10.3389/fimmu.2022.890710>  
PMID:35734175
43. Li Y, Wang SM, Li X, Lv CJ, Peng LY, Yu XF, Song YJ, Wang CJ. Pterostilbene pre-treatment reduces LPS-induced acute lung injury through activating NR4A1. *Pharm Biol.* 2022; 60:394–403.  
<https://doi.org/10.1080/13880209.2022.2034893>  
PMID:35271397
44. Duan J, Xiang L, Yang Z, Chen L, Gu J, Lu K, Ma D, Zhao H, Yi B, Zhao H, Ning J. Methionine Restriction

- Prevents Lipopolysaccharide-Induced Acute Lung Injury via Modulating CSE/H<sub>2</sub>S Pathway. *Nutrients*. 2022; 14:322.  
<https://doi.org/10.3390/nu14020322>  
PMID:[35057502](https://pubmed.ncbi.nlm.nih.gov/35057502/)
45. Thompson BT, Chambers RC, Liu KD. Acute Respiratory Distress Syndrome. *N Engl J Med*. 2017; 377:562–72.  
<https://doi.org/10.1056/NEJMr1608077>  
PMID:[28792873](https://pubmed.ncbi.nlm.nih.gov/28792873/)
46. Lestari SR, Atho'llah MF, Christina YI, Rifa'i M. Single garlic oil modulates T cells activation and proinflammatory cytokine in mice with high fat diet. *J Ayurveda Integr Med*. 2020; 11:414–20.  
<https://doi.org/10.1016/j.jaim.2020.06.009>  
PMID:[32798194](https://pubmed.ncbi.nlm.nih.gov/32798194/)
47. Maeda A, Hayase N, Doi K. Acute Kidney Injury Induces Innate Immune Response and Neutrophil Activation in the Lung. *Front Med (Lausanne)*. 2020; 7:565010.  
<https://doi.org/10.3389/fmed.2020.565010>  
PMID:[33330525](https://pubmed.ncbi.nlm.nih.gov/33330525/)
48. Goodman RB, Pugin J, Lee JS, Matthay MA. Cytokine-mediated inflammation in acute lung injury. *Cytokine Growth Factor Rev*. 2003; 14:523–35.  
[https://doi.org/10.1016/s1359-6101\(03\)00059-5](https://doi.org/10.1016/s1359-6101(03)00059-5)  
PMID:[14563354](https://pubmed.ncbi.nlm.nih.gov/14563354/)
49. Reutershan J, Vollmer I, Stark S, Wagner R, Ngamsri KC, Eltzschig HK. Adenosine and inflammation: CD39 and CD73 are critical mediators in LPS-induced PMN trafficking into the lungs. *FASEB J*. 2009; 23:473–82.  
<https://doi.org/10.1096/fj.08-119701>  
PMID:[18838482](https://pubmed.ncbi.nlm.nih.gov/18838482/)
50. Grommes J, Soehnlein O. Contribution of neutrophils to acute lung injury. *Mol Med*. 2011; 17:293–307.  
<https://doi.org/10.2119/molmed.2010.00138>  
PMID:[21046059](https://pubmed.ncbi.nlm.nih.gov/21046059/)
51. Abraham E. Neutrophils and acute lung injury. *Crit Care Med*. 2003; 31:S195–9.  
<https://doi.org/10.1097/01.CCM.0000057843.47705.E8>  
PMID:[12682440](https://pubmed.ncbi.nlm.nih.gov/12682440/)
52. Lee WL, Downey GP. Neutrophil activation and acute lung injury. *Curr Opin Crit Care*. 2001; 7:1–7.  
<https://doi.org/10.1097/00075198-200102000-00001>  
PMID:[11373504](https://pubmed.ncbi.nlm.nih.gov/11373504/)
53. Li Q, Verma IM. NF-kappaB regulation in the immune system. *Nat Rev Immunol*. 2002; 2:725–34.  
<https://doi.org/10.1038/nri910>  
PMID:[12360211](https://pubmed.ncbi.nlm.nih.gov/12360211/)
54. Martinon F, Burns K, Tschopp J. The inflammasome: a molecular platform triggering activation of inflammatory caspases and processing of proIL-beta. *Mol Cell*. 2002; 10:417–26.  
[https://doi.org/10.1016/s1097-2765\(02\)00599-3](https://doi.org/10.1016/s1097-2765(02)00599-3)  
PMID:[12191486](https://pubmed.ncbi.nlm.nih.gov/12191486/)
55. Ning L, Wei W, Wenyang J, Rui X, Qing G. Cytosolic DNA-STING-NLRP3 axis is involved in murine acute lung injury induced by lipopolysaccharide. *Clin Transl Med*. 2020; 10:e228.  
<https://doi.org/10.1002/ctm2.228>  
PMID:[33252860](https://pubmed.ncbi.nlm.nih.gov/33252860/)